Intracranial strain and displacements from impacts to a helmeted deformable headform

S. Xu[1], S. Dutrisac[1], S. Ouellet[2], and **O.E. Petel**[1]

[1]Carleton University, 1125 Colonel By Drive, Ottawa, ON, Canada
oren.petel@carleton.ca
[2]DRDC Valcartier, 2459 Pie-XI Blvd North, Quebec, QC, Canada

Abstract. Novel techniques and tools are needed in helmet performance and injury evaluation. Advances in headforms have been made in recent years, with a shift towards the use of deformable skull and brain surrogates. The development of these headforms has also brought about the integration of new diagnostic capabilities that reach beyond the classic rigid body mechanics approach to injury evaluation. The majority of these diagnostic systems provide only discrete measurements within the headform, that are dependent on the choice of gauge placement. In the present work, we demonstrate advances that have been made in making temporally-resolved full-field intracranial strain and displacement measurements within the surrogate brain of a deformable headform during an impact event. The approach involves the use a custom-built *in situ* high-speed X-ray system. Radiopaque contrast media were integrated into the surrogate to enable tracking of the displacement fields that can then be used to calculate intracranial strain. The measurements presented in this work were taken along a parasagittal plane within the headform. The interaction between the helmet and headform as well as the deformation fields measured within the brain surrogate show tremendous potential for future use in equipment performance evaluation, returning tissue-level metrics that are related to injury mechanisms of traumatic brain injury.

1. INTRODUCTION

Mild-Traumatic Brain Injury (mTBI), whether caused exposure to blast or a direct impact event, remains a primary non-lethal health concern. A recent study of the epidemiology of mTBI among military veterans from the Iraq and Afghanistan war era found that approximately 15.1% had sustained an mTBI relating to their service, of which one third were due to blast exposure, while nearly half were due to blunt impact events (e.g., object hitting head or falls) [1]. Reducing the incidence of these injuries will require improvements to personal protective headgear. Aside from their ballistic performance, military helmets are also subjected to a variety of performance characterization tests for their blunt impact performance [2]. The approaches used to qualify their response are similar to testing methodologies for athletic headgear [3-5]. Those testing procedures, typically involving drop-testing of a helmeted headform onto an anvil in different orientations and measuring the resulting acceleration profiles, focused on reducing the risk of focal injuries (e.g., skull fracture or severe brain trauma) from an impact [3,4]. Given the known link between rotational acceleration of the head and mTBI risk [6,7], linear impactor test protocols have recently been used to set additional performance criteria on athletic headgear [6]. These test protocols have yet to be mirrored in military helmet impact testing. Despite the continued modernization of testing standards, they are not yet able to directly address tissue-level metrics in their testing platforms, focusing exclusively on the rigid body mechanics of the head. Assessing injury risk from these tests has relied on either impact severity criteria [8-11] or coupling the testing protocols to computational models validated against limited cadaveric datasets [12,13]. In the present work, we present the first efforts to establish a deformation-based measurement within a helmeted headform to describe the performance of helmet.

Although current testing procedures use rigid headforms, there have been a considerable effort to design headforms with deformable structures that provide for various modal and inertial responses [14-17]. Several advanced tissue-simulating headforms with elastomeric brain surrogates have been designed in recent years to investigate blast-induced traumatic brain injury (bTBI). These headforms have all been optimized and calibrated for bTBI events. The brain surrogates of these headforms providing researchers with new opportunities to extract local measurements at the brain level. As these headforms improve in their biofidelity, the diagnostic capabilities must be adapted to take advantage of the opportunities for tissue-level metrics to be captured. The headforms have thus far been primarily limited to measurements of global head kinematics and discrete pressure measurements [17]. As such, the full potential of these tissue-simulating headforms has yet to be achieved. Thus, there is a need for new testing methodologies that directly investigate full-field tissue-level metrics of relevance to mTBI, such as brain displacement and deformation.

https://doi.org/10.52202/078352-0051

Monitoring full-field tissue-level metrics associated with blunt trauma required a new diagnostic approach to investigating the headform. The approach chosen involves the use of a custom-built *in situ* high-speed X-ray (HSXR) cinematography system, capable of high capture rates through the headform, to monitor radiopaque marker motion within the headform to determine intracranial displacement and deformation [18]. In the present study, we use this approach to determine the response of the surrogate brain to a frontal impact on a tactical military helmet. The focus was to determine the response of the brain surrogate. This new helmet evaluation technique, once adequately calibrated, represents an opportunity to use tissue-level deformation metrics to evaluate helmet performance and head trauma risks associated with head impacts. At this time, this headform is undergoing a calibration in relation to cadaveric datasets using the same physical setup, however this phase of the work is ongoing and the purpose of the present study is to show the early development of this capability.

2. EXPERIMENTAL CONFIGURATION

The BIPED headform, a thorough description of which can be found in [16,17], was used in the present study. The headform features several intracranial anatomical structures, such as a cerebellum, artificial cerebrospinal fluid (CSF), and falx and tentorium membrane simulants. For the present work, the brain surrogate, which was cast from Sylgard 527, was altered by the insertion of radiopaque markers during the casting process. The markers were placed along a parasagittal plane, 15 mm from the midsagittal plane. Marker composition included a mixture of a thermoplastic gel (Humimic gel #4) with barium sulphate powder (60% by mass). The markers were cylindrical with a 1.5-mm diameter and 2-mm length. Once the brain was sealed within the headform, water was flushed through the intracranial spaces to act as CSF and ensure that the headform was fully perfused prior to testing. During testing, a static pressure of 1 m of H_20 was maintained on the fluid to replicate the vasculature and intracranial repressurization used in prior cadaver studies [12].

For the impact tests, the headform was placed on a linear impactor platform (Cadex) and subjected to a series frontal impacts from a 13.13 kg ram to test the response of the Viper helmet (Galvion). The end cap of the impacting ram was a steel front plate backed by a rubber to simulate the anvil used in military helmet drop testing. The headform was attached to a neck-form variation on the Hybrid III neck that does not have a directional bias [19]. The neck was pre-tensioned to 1ft-lb. The data presented in this paper was generated by two impacts on the same helmeted headform that was subjected to impacts at speeds of 3.15 m/s and 3.54 m/s. These impact conditions correspond to impact energies of approximately 65J and 82J, respectively. The headform was inclined at an angle of 15° for both of these impacts. The headform acceleration history was recorded on a rigidly attached neck extension with an attached DTS 6DX Pro accelerometer and then translated to the centre of gravity of the headform. A photograph of the headform, mounted to a linear impactor table, prior to a test is shown in Figure 1.

Figure 1. Photograph of the helmeted headform with the end cap of the linear impactor visible.

The images captured by the HSXR were processed using an open-source Matlab-based Digital Image Correlation (DIC) script, NCorr [20] to determine the displacement and deformation fields within

https://doi.org/10.52202/078352-0051

the headform. For the DIC analysis, a speckle radius range of 7-10 pixels, a subset radius of 25 pixels, a strain radius of 15 pixels and a subset spacing of 2 pixels were used to generate the results.

3. RESULTS

The linear and rotational acceleration at the centre of gravity of the headform for the impact are shown in Figure 2a and 2b, respectively. The headform was subjected to peak linear and rotational accelerations of 50 g and 2,280 rad/s^2 and 65 g and 3,300 rad/s^2 for the 65J and 82J impacts, respectively. These two impact conditions resulted in peak resultant rotational rates of the headform of 15.8 rad/s and 17.8 rad/s, respectively. X-ray images of this impact were captured with our custom HSXR at a frame rate of 5,000 fps. A series of images captured over the first 70 ms of the 82J impact event are shown at 10 ms intervals in Figure 3. The corresponding shear strain fields in the head fixed reference frame at the associated time intervals are also shown in Figure 3. Note that the strains are shown in a reference frame fixed to the initial skull position in the initial frame of the sequence. The displacement paths of the brain surrogate from this impact, in the skull-fixed reference frame, are shown in Figure 3. These paths are not tracking the displacement of a single marker within the surrogate, but rather are related to the motion paths of pixel subsets. Figure 5 shows the resultant displacement histories of the points from Figure 4 over the first 70 ms following this impact. These results can also be plotted out in the same fashion to demonstrate the shear strain fields within the headform, as shown in Figure 6.

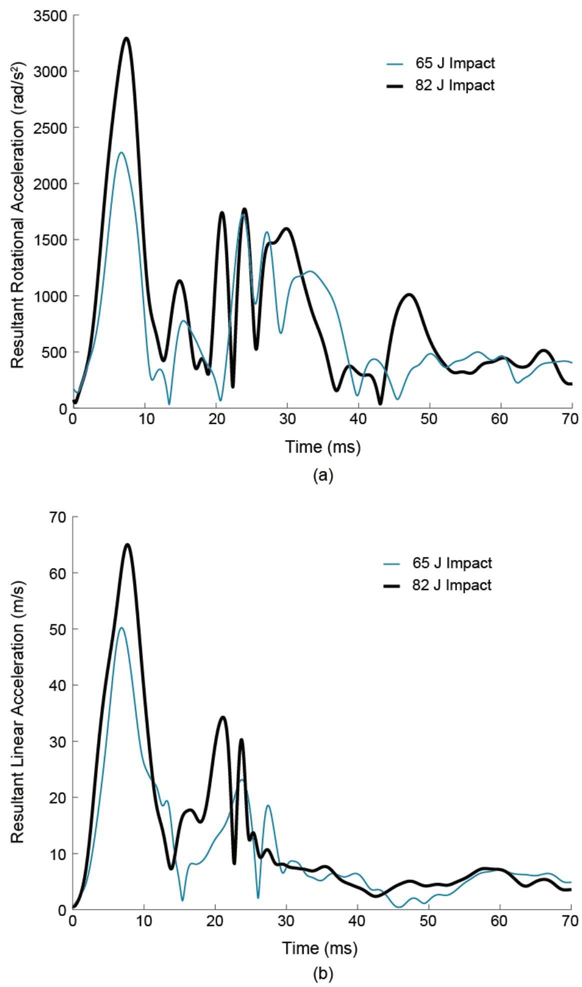

Figure 2. (a) Linear and (b) Rotational acceleration profiles of the headform at its centre of gravity.

https://doi.org/10.52202/078352-0051

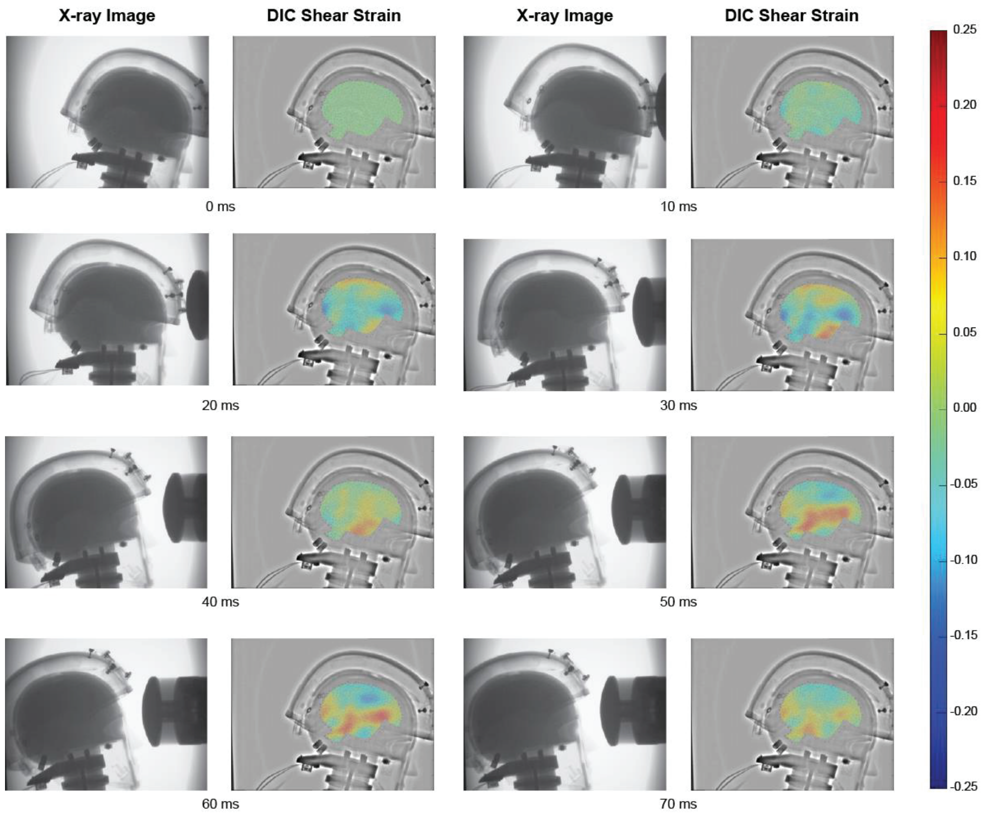

Figure 3. The original X-ray images of the headform impact beside the corresponding X-ray DIC images of the shear strain fields calculated from the image.

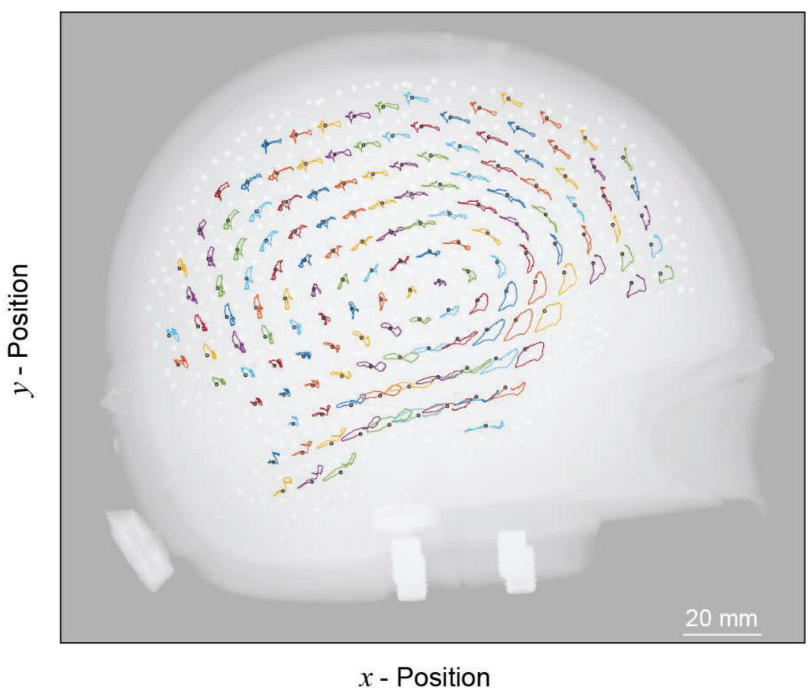

Figure 4. Complete displacement paths of the brain surrogate over a period of 70 ms following impact. The circles mark the start of the paths, and each path has a different colour for clarity.

https://doi.org/10.52202/078352-0051

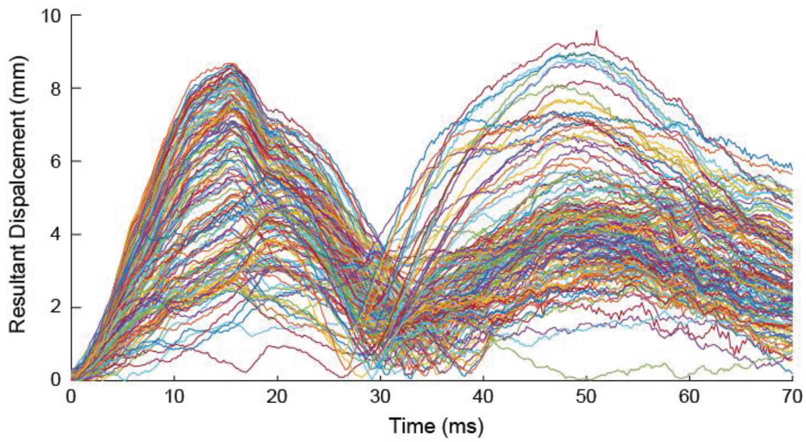

Figure 5. The resultant displacement field within the brain.

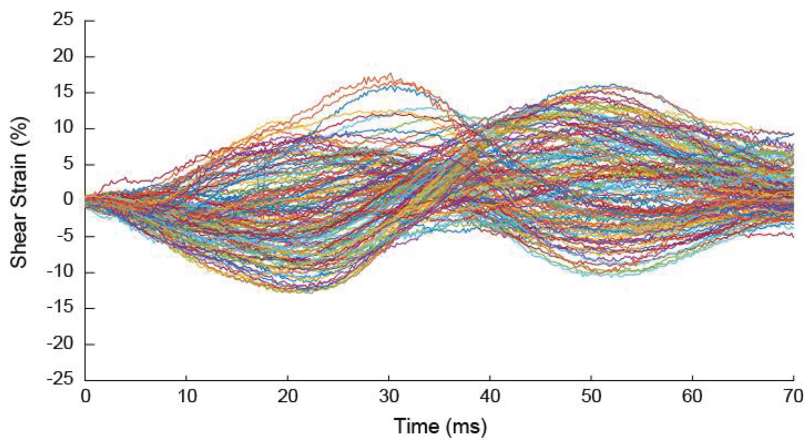

Figure 6. Shear strain histories of individual points within the brain surrogate.

4. DISCUSSION

The results shown in Figures 3 through 6 demonstrate the amount of information relating to tissue-level metrics associated with injury outcomes that can be gleaned from this experimental technique. There are several features in the results that are worthy of note. In Figure 4, there are distinct motion patterns that develop as a result of the impact. The overall motion of the brain surrogate results in a clear rotation of the brain about its centre of gravity. The temporal region is subjected to broader lateral motion than other regions of the brain. When we examine these features in the resultant displacement plots of Figure 5, which are not directional, we see similar features. The displacement magnitude of the brain is notably region dependent. For instance, the peak displacement in the parietal and occipital regions had peak displacements of approximately 4 mm from their initial positions, while the motion in the frontal, temporal, cerebellum regions was notably larger, on the order of 6-7 mm. The displacement histories in Figure 5 also shows a double peak in the displacement field. This is related to the initial motion, change of direction and slowing of the brain, with the second displacement peak coinciding with the full extent of motion of the head. While the primary phase of head acceleration occurs in the first 15 ms of the impact, brain motion continued to occur over a considerably longer timescale. Furthermore, the second displacement peak was slightly larger than the primary peak in certain regions of the brain, such as the temporal region. While the displacement histories represent the resultant motion and are thus non-directional, comparing these paths to Figure 4 shows that the total deviation of a given marker was

https://doi.org/10.52202/078352-0051

approximately double the peaks seen in Figure 5, as the markers first moved in one direction, then reversed their course.

This motion reversal had a notable effect on the shear strain field calculated within the head, as seen in Figure 3. The shear strain histories show a shear reversal, which is essentially a reversal in the distortion angle of the tissues during the impact event. The inversion of the strains was seen in every region of the brain. The peak shear strain for the impact was on the order of 18% and occurred in the temporal region. This is consistent with the strain fields shown in Figure 3. The parietal, occipital, and cerebellum regions saw the lowest strains. Of particular interest was the response in the frontal and temporal regions, where the strain rate associated with the second strain peak was significantly higher than the initial strain rate associated with the impact. The timing of this inversion is unrelated to the global kinematic response of the head and demonstrates the effect of the decoupled motion of the brain and skull.

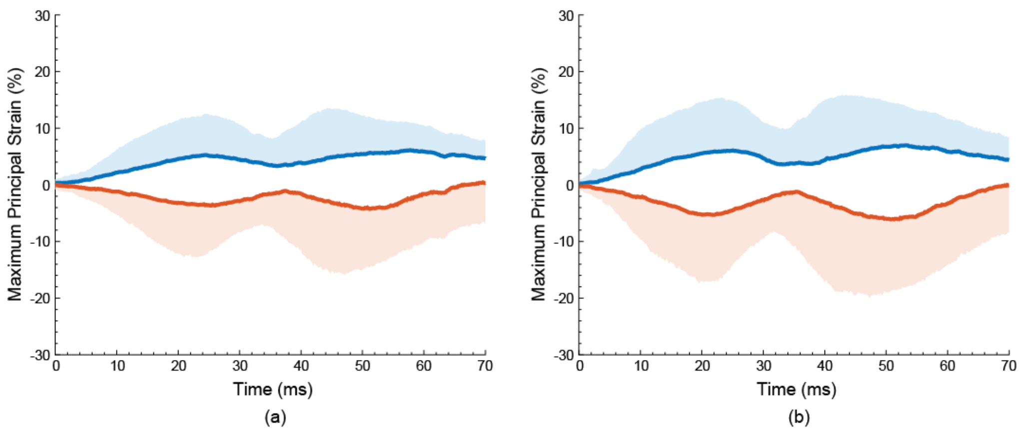

Figure 7. Maximum Principal Strain (MPS) profiles within the brain surrogate for the (a) 65J impact and the (b) 82J impact. The thick lines represent the mean MPS within the brain surrogate, while the shaded bounds represent the 95th percentile MPS values.

The results of the tests were plotted to show the Maximum Principal Strain (MPS) values associated within the brain surrogate for the two impact conditions in Figure 7. The mean and 95th percentile values are shown for tensile and compressive MPS. While the trends in the MPS profiles were the similar under both impact conditions, this comparison showed that there were notable differences in the peak strains within the surrogate, demonstrating that the headform is sensitive enough to measure strain differences associated with increasing impact severity. Thus, this measurement capability has potential as a future helmet performance evaluation tool, returning intracranial strain response measurements.

While there is still work to be done to ensure the biofidelic response of this headform lies within an acceptable human performance corridor, particularly in its impact response, the methods developed in this work are broadly applicable to the field of injury biomechanics. The tissue-level responses that were measured in the present work present a new avenue for research in injury biomechanics, returning metrics that can be directly related to suspected injury mechanisms, such as brain tissue strain. While the datasets currently generated by this headform cannot be directly linked to clinical outcomes, the long-term objective will be such a validation to allow its use as a helmet testing and evaluation platform.

5. CONCLUSIONS

A new testing approach for helmet evaluation has been presented, demonstrating its ability to generate high temporal and spatial resolution tissue-level displacement and strain fields across the entire headform model. A tactical military helmet was tested under a linear impact load and the resulting strain and displacement fields were measured. Using this headform and DIC technique, we have demonstrated some interesting dynamics within the brain surrogate relating to the rotation and inversion of the tissue

https://doi.org/10.52202/078352-0051

distortion field at high strain rate. Further calibration and validation of this headform is warranted and will help it develop into a useful tool for helmet performance evaluation.

Acknowledgments

The authors acknowledge funding support from CIHR-NSERC under grant CHRPJ 508414-17 and financial support for X-ray infrastructure from the Canadian Foundation for Innovation and the Ontario Research Fund under project 39233. The authors thank William Bedard for his assistance in preparing the headform.

References

[1] Lindquist, L.K., Love H.C., and Elbogen, E.B., J Neuropsychiatry Clin Neurosci, 2017; 29(3); 254-259.
[2] Hopping, J. A., Bass, C., Shridharani, J., Perritt, C., Haynes, N., & Masters, K. (2010). Methodologies for blunt trauma assessment in military helmets. Proceedings of the Personal Armour System Symposium; 2010; Quebec City, Canada.
[3] National Operating Committee on the Standards for Athletic Equipment (NOCSAE). Standard Test Method and Equipment Used in Evaluating the Performance Characteristics of Protective Headgear/Equipment, 2012.
[4] ASTM, "Standard Test Methods for Equipment and Procedures Used in Evaluating the Performance Characteristics of Protective Headgear," American Society for Testing and Materials, pp. Standard F1446-13, 2013.
[5] National Operating Committee on the Standards for Athletic Equipment (NOCSAE). Standard Pneumatic Ram Test Method and Equipment Used in Evaluating the Performance Characteristics of Protective Headgear and Face Guards, 2018.
[6] Pellman E.J., Viano D.C., Tuck A.M., Casson I.R., and Waeckerle J.F., Neurosurg, 2003; 53(4); 799-814.
[7] Rowson S., Duma S.M., Beckwith J.G., Chu J.J., Greenwald R.M., Crsico J.J., Brolinson P.G., Duhaime A.-C., McAllister T.W., and Maerlender A.C., Ann Biomed Eng, 2012; 40(1); 1–13.
[8] Gadd C.W., Use of a Weighted-Impulse Criterion for Estimating Injury Hazard. SAE Technical Paper, 1966.
[9] Newman J., Shewchenko N., and Welbourn E., Stapp Car Crash J, 2000, 44:215-247.
[10] Takhounts E.G., Craig M.J., Moorhouse K., McFadden J., and Hasija V., Stapp Car Crash J, 2013; 57;243–266.
[11] Gabler L.F., Crandall J.R., and Panzer M.B, Ann Biomed Eng, 2018; 46(7);972-985.
[12] Hardy W.N., Foster C.D., Mason M.J., Yang K.H., King A.I., and Tashman S., Stapp Car Crash J., 2001; 45; 337–368.
[13] Hardy W.N., Mason M.J., Foster C.D., Shah C.S., Kopacz J.M., Yang K.H., King A.I, Bishop J., Bey M., Anderst W., et al, Stapp Car Crash J., 2007; 51;17-80.
[14] Ganpule S., Mechanics of blast loading on PMHS and surrogate heads in the study of traumatic brain injury using experimental and computational approaches. Ph.D. Dissertation, University of Lincoln Nebraska, 2013.
[15] Merkle A., Wing I.D., Armiger R.A., Carkhuff B.G., and Roberts J.C., Proceedings of ASME International Mechanical Engineering Congress, Lake Buena Vista, Florida, USA, 2009.
[16] Ouellet S., Bir C., and Bouamoul A., Proceedings of the Personal Armour System Symposium; 2014; Cambridge, UK.
[17] Ouellet S and Philippens M., Shock Waves, 2018; 28; 19-36.
[18] Petel O.E., Diagnostic for in situ deformation and strain measurements applicable to traumatic internal injury investigation and prevention. USPTO Patent 9,826,954, 2015.
[19] Walsh E.S., Kendall M., Post A., Meehan A., and Hoshizaki T.B., Sports Eng., 2018; 21;479–485.
[20] Blaber J., Adair B., and Antoniou A., Exp. Mech., 2015; 55;1105-1122.

 https://doi.org/10.52202/078352-0051